Supplemental Material

Identification of Mn(II)-oxidizing bacteria from a low pH contaminated former uranium mine

Denise M. Akob[1,2 *], Tsing Bohu[1], Andrea Beyer[1†], Franziska Schäffner[3], Matthias Händel[3], Carol A. Johnson[4], Dirk Merten[3], Georg Büchel[3], Kai Uwe Totsche[3], and Kirsten Küsel[1,5]

[1]Institute of Ecology, Friedrich Schiller University Jena, Dornburger-Straße 159, 07743 Jena, Germany

[2]Present address: U.S. Geological Survey, National Research Program, 12201 Sunrise Valley Drive, MS 430, Reston, VA 20192 USA

[3]Institute of Geosciences, Friedrich Schiller University Jena, Burgweg 11, 07749 Jena, Germany

[4]Department of Geosciences, Virginia Tech, 4044 Derring Hall, Blacksburg, VA 24061, USA

[5]German Centre for Integrative Biodiversity Research (iDiv) Halle-Jena-Leipzig, Deutscher Platz 5e, 04103 Leipzig, Germany

[†]Present address: Institute for Microbiology, Friedrich Schiller University Jena, Neugasse 25, 07743 Jena, Germany

*Corresponding author:
Dr. Denise M. Akob
U.S. Geological Survey
12201 Sunrise Valley Drive, MS 430
Reston, VA 20192 USA
Phone: 703-648-5819
E-mail: dakob@usgs.gov

Supplemental Material Description

Supplemental material showing the location of study sites within the former uranium-mining district Ronneburg (Fig. S1), geochemistry of site GTF (Fig. S2), FTIR spectra of agar medium, AB_14 biomass, and synthetic birnessite (Fig. S3), and TEM EDX of biogenic Mn oxides (Fig. S4), structural comparison between Mn oxides formed in this study and those from the literature (Table S1), statistical analyses of 16S rRNA gene clone libraries from site GTF (Table S2).

Figure S1: Map of the former uranium-mining district Ronneburg, Germany showing the locations of sampling sites GTF (Gessenwiese Test Field), B (Gessen Creek bank soil), and R3 (Gessen Creek sediment). The inset for site GTF shows a soil core with the three layers sampled: Top, Mn-rich layer and Bottom. At the Gessen Creek site B, soils from horizon BElc were sampled. Map was modified from Fabisch et al. (1). Photo credits: site GTF: T. Bohu, site B: S. Bischoff, and site R3: M. Fabisch.

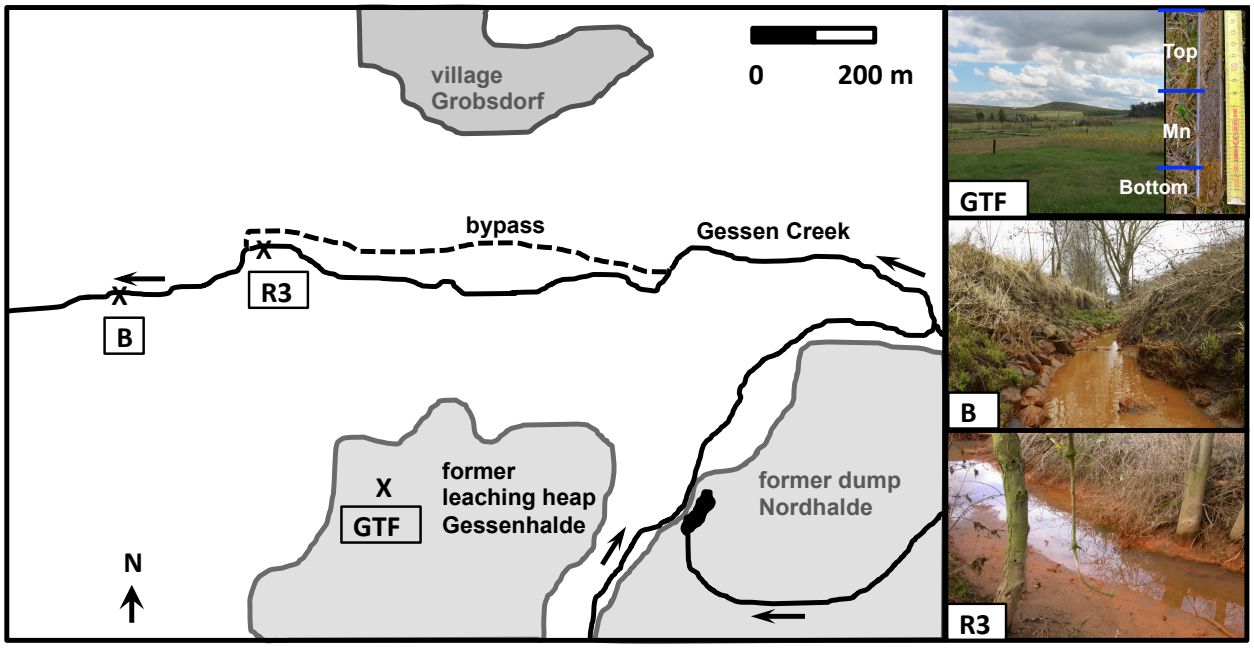

Figure S2: Metal concentrations of the sediment, in µg/g (filled areas), along the GTF subsurface profile and metal concentrations in the pore water, in µM (circles), of the water-saturated layers.

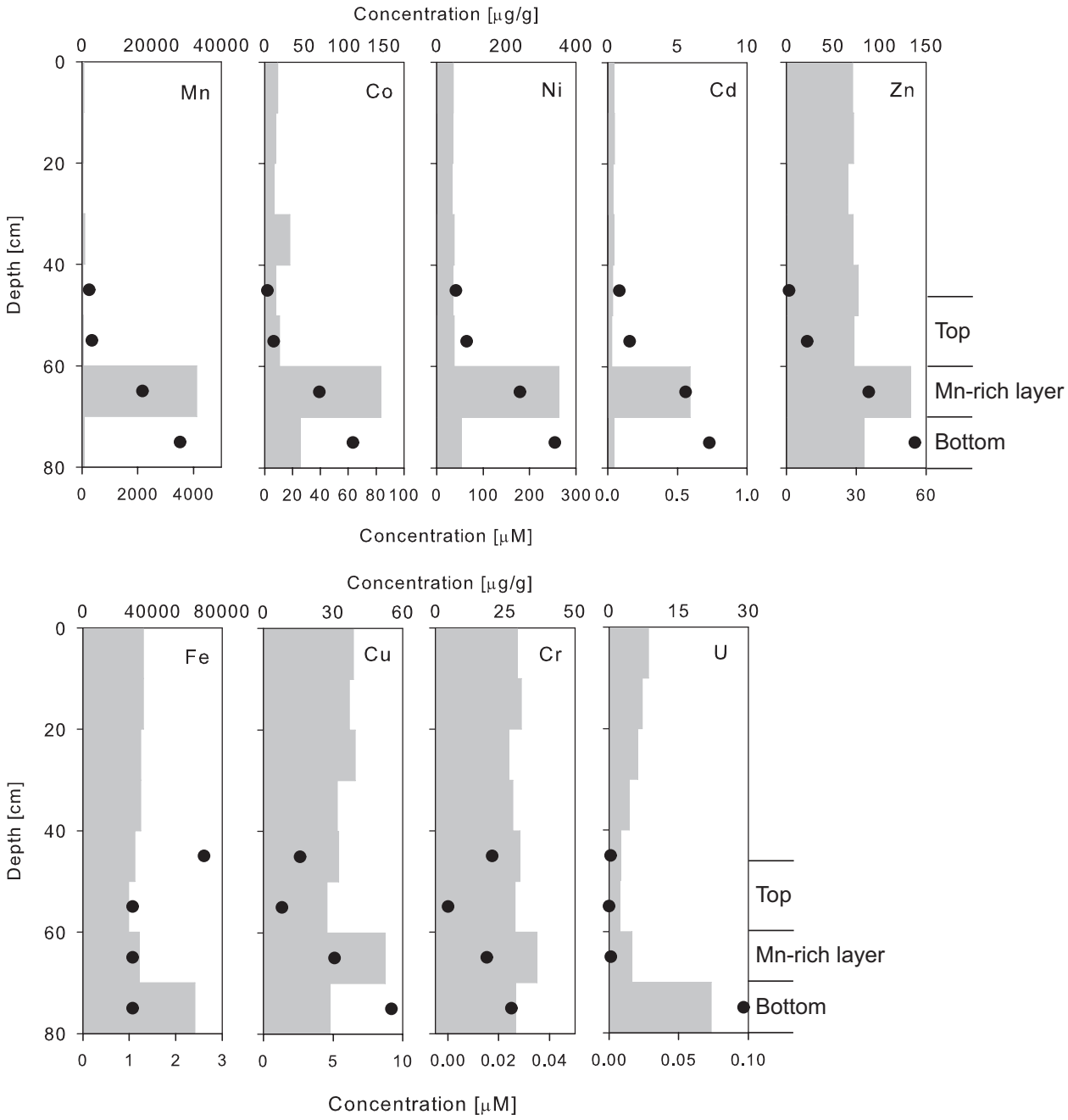

Figure S3: FTIR spectra of (a) agar medium, (b) AB_14 biomass, and (c) synthetic birnessite.

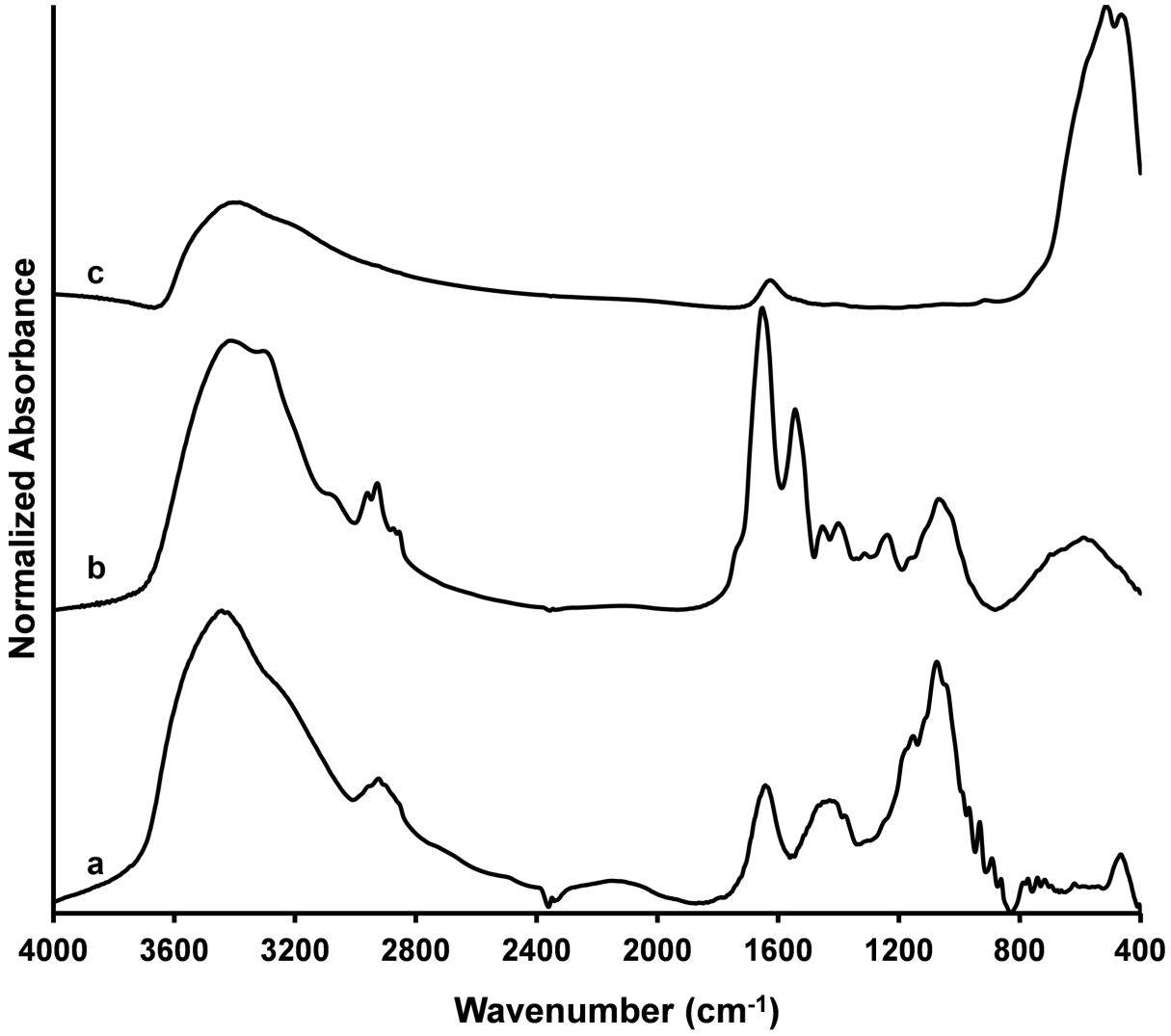

Figure S4: TEM EDX of Mn oxides in resin-embedded, ultramicrotomed cultures of (a) AB_14, same area as in Figure 4f and (b) AB_18, similar area to Figure 4c. C, P and Si are from the resin, Cu is from the TEM support grid; Pb and U are from stains used to accentuate cell features (staining procedures described in the Experimental Procedures). Therefore, these particular minerals shown in Figure 4 are Mn oxides with no Fe.

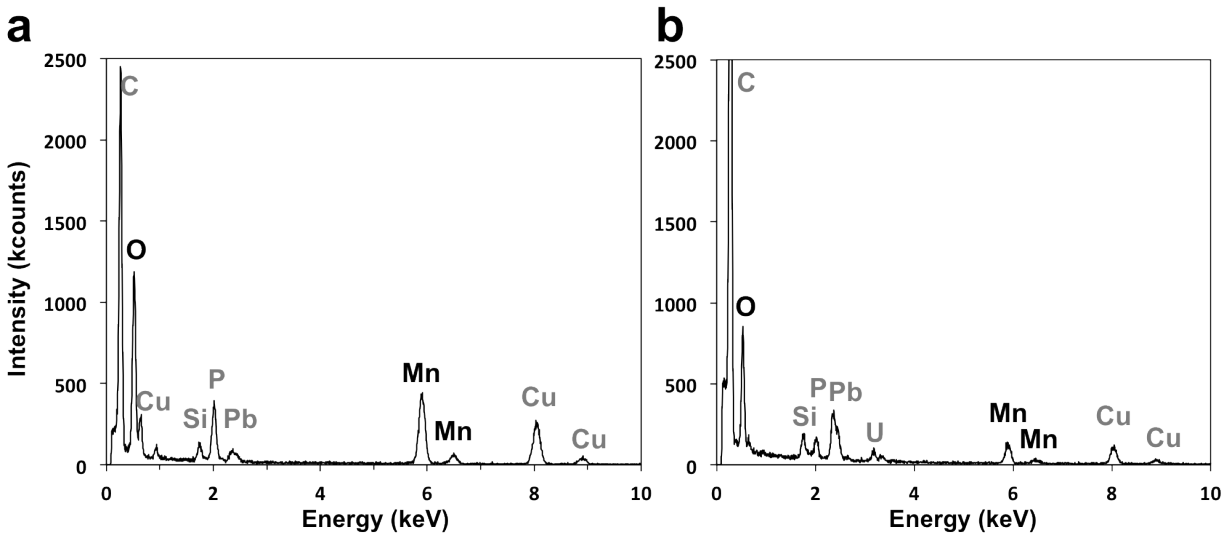

Table S1. Structural comparison between Mn oxides formed in this study and those from the literature. D-spacings (Å) are from selected area diffraction (SAED) patterns in Figure 3c, e, f. Values from the literature do not represent all of the possible d-spacings.

AB_18	AB_14				
SAED (c) d (Å)	SAED (e) d (Å)	SAED (f) d (Å)	Birnessite[a] d (Å)	Birnessite[b] d (Å)	Todorokite[c] d (Å)
			7.14	7.09	7.06
	6.64	6.49			6.55
	5.72	5.68		5.6	
	3.91				4.17
	3.74				
			3.57	3.56	3.54
	3.35	3.24			
3.01		2.96			3.08
	2.86				
		2.51	2.52	2.51	
			2.48		
2.39			2.43	2.42	2.43
	2.27		2.32	2.26	2.32
			2.22		2.22
	2.15		2.15	2.15	2.12
2.00	2.00	2.03		2.09	2.00
1.92	1.91	1.93		1.94	
	1.86		1.87	1.86	1.87
	1.68	1.72		1.66	
	1.65		1.63	1.63	
1.60		1.60		1.63	
1.53		1.48		1.47	

a. Synthetic, PDF (Powder Diffraction File) 00-043-1456 (2); synthetic, PDF 01-072-6745 (2, 3)

b. Synthetic, PDF 00-23-1046 (2)

c. Natural mineral, PDF 00-038-0475 (2)

Definitive determination of the exact mineral phases in these samples was difficult, in part because there is a lack of good quality diffraction data for Mn oxides, the birnessite structure can vary in nature, and many of the d-spacings are common within different Mn oxides. Multiple phases can also occur in a single particle (4). Sample preparation can also be an issue, and in this case the AB_18 and AB_14 samples were embedded in resin making them neither dehydrated

nor hydrated with water. Instead, organic molecules could fill the interlayer, either shrinking or expanding that largest d-spacing (interlayer spacing). The resin that was used, araldite, was not stable under the electron beam at a wide range of instrument conditions, and neither were the Mn oxides. Electron diffraction data had to be collected in 30s or less, otherwise crystallinity was lost, indicating possible mineral transformation. Therefore, the combination of EDS and SAED data only allows us to conclude that crystalline Mn oxides were produced.

Table S2: Statistical analyses of 16S rRNA gene clone libraries for GTF subsurface layers Top, Mn-rich and Bottom.

Sample	No. sequences	No. OTUs[a]	Coverage	Chao1[b]	Shannon diversity (H')	Simpsons diversity (1/D)
Top	85	51	0.58	108	3.59	26.84
Mn	61	30	0.72	47	3.10	20.80
Bottom	63	19	0.86	55	2.57	11.63

a. OTU, operational taxonomic unit at a distance of 0.03.

b. Chao1, Chao1 species richness

References

1. **Fabisch, M., F. Beulig, D. M. Akob, and K. Küsel.** 2013. *Gallionella*-related bacteria outnumber other iron oxidizing bacteria even at pH 4.4 or at high heavy metal concentrations. Frontiers in Microbiology **4:**390.

2. **ICDD.** 2010. PDF-2 2010 (Database), edited by Dr. Soorya Kabekkodu. International Centre for Diffraction Data, Newtown Square, PA, USA

3. **Lanson, B., V. A. Drits, Q. Feng, and A. Manceau.** 2002. Structure of synthetic Na-birnessite: Evidence for a triclinic one-layer unit cell. Am. Mineral. **87:**1662–1671.

4. **Rask, J. H., and P. R. Buseck.** 1986. Topotactic relations among pyrolusite, manganite, and Mn5O8: A high-resolution transmission electron microscopy investigation. Am. Mineral. **71:**805-814.